



Molecular Cage Assembly by Sn—O—Sn Bridging of Di-, Tri- and Tetranuclear Organotin Tectons: Extending the Spacing in Double Ladder Structures

Irán Rojas-León⁺,^[a, c] G. Gómez-Jaimes⁺,^[a, b] Pedro Montes-Tolentino,^[a] Wolf Hiller,^[c] Hazem Alnasr,^[c] Braulio Rodríguez-Molina,^[d] Irán F. Hernández-Ahuactzi,^[e] Hiram Beltrán,^[b, f] Klaus Jurkschat,^{*[c]} and Herbert Höpfl^{*[a]}

Abstract: Hydrolysis reactions of di- and trinuclear organotin halides yielded large novel cage compounds containing Sn—O—Sn bridges. The molecular structures of two octanuclear tetraorganodistannoxanes showing double-ladder motifs, viz., $[(\text{Me}_3\text{SiCH}_2(\text{Cl})\text{SnCH}_2\text{YCH}_2\text{Sn}(\text{OH})\text{CH}_2\text{SiMe}_3)_2(\mu\text{-O})_2]_2$ [**1**, $\text{Y} = p\text{-}(\text{Me})_2\text{SiC}_6\text{H}_4\text{-C}_6\text{H}_4\text{Si}(\text{Me})_2$] and $[(\text{Me}_3\text{SiCH}_2(\text{I})\text{SnCH}_2\text{YCH}_2\text{Sn}(\text{OH})\text{CH}_2\text{SiMe}_3)_2(\mu\text{-O})_2]_2 \cdot 0.48 \text{I}_2$ [**2**·0.48 I₂, $\text{Y} = p\text{-}(\text{Me})_2\text{SiC}_6\text{H}_4\text{-C}_6\text{H}_4\text{Si}(\text{Me})_2$], and the hexanuclear cage-compound $1,3,6\text{-C}_6\text{H}_3(p\text{-C}_6\text{H}_4\text{Si}(\text{Me})_2\text{CH}_2\text{Sn}(\text{R})_2\text{OSn}(\text{R})_2\text{CH}_2\text{Si}(\text{Me})_2\text{C}_6\text{H}_4\text{-}p)_3\text{C}_6\text{H}_3\text{-}1,3,6$ (**3**, $\text{R} = \text{CH}_2\text{SiMe}_3$) are reported. Of these, the co-crystal **2**·0.48 I₂ exhibits the largest spacing of 16.7 Å reported to date for distannoxane-based double ladders. DFT calculations for the hexanuclear cage and a related octanuclear congener accompany the experimental work.

Introduction

Metal-coordination driven self-assembly has many facets and is among the fields most explored in modern chemistry.^[1,2] Within the panorama of metal-organic aggregates that can be achieved via this method, macrocycles and cages^[3–8] are

important targets because of potential applications in guest recognition, separation, storage, transport, catalysis, among others.^[9–12] For the assembly of cage-type structures, preshaped building blocks (tectons) are needed to fulfil the geometric requirements for obtaining the desired supramolecular aggregate.^[13–17]

So far, cage compounds based on discrete tin metal centres, viz., Sn^{+II} and Sn^{+IV}, have been little explored^[18–19] and there are only few reports on related compounds using mononuclear organotin moieties.^[20–22] Cages derived from more complex tin building units are also known and can be divided into two categories. In the first category, the tectons are secondary building blocks^[17] based on inorganic clusters such as di- or oligonuclear organotin oxides, sulfides and selenides,^[23–25] which are then interconnected by diverse inorganic and organic ligands.^[26–29] In the second category, organotin compounds with two or more tin centres in a single building block and linked through an organic spacer are used for further connection with the ligands.^[30–33] Organotin halides are susceptible to the formation of Sn—O—Sn bridges (Scheme 1).^[34–35] Accordingly, if the tin atoms in the organotin oxides given in Scheme 1 are replaced by di- or oligonuclear organotin tectons, more complex assemblies having macrocyclic, cage-type or polymeric structures might be achieved. In other words, the transformation by hydrolysis of oligonuclear organotin halides into the

[a] Dr. I. Rojas-León,⁺ G. Gómez-Jaimes,⁺ Dr. P. Montes-Tolentino, Prof. Dr. H. Höpfl
 Centro de Investigaciones Químicas
 Instituto de Investigación en Ciencias Básicas y Aplicadas
 Universidad Autónoma del Estado de Morelos
 Av. Universidad 1001, Cuernavaca, Morelos 62209 (México)
 E-mail: hhopfl@uaem.mx

[b] G. Gómez-Jaimes,⁺ Prof. Dr. H. Beltrán
 Departamento de Ciencias Naturales, DCNI
 Universidad Autónoma Metropolitana Cuajimalpa
 Ciudad de México 05370 (México)

[c] Dr. I. Rojas-León,⁺ Prof. Dr. W. Hiller, Dr. H. Alnasr, Prof. Dr. K. Jurkschat
 Fakultät für Chemie und Chemische Biologie
 Technische Universität Dortmund
 44221 Dortmund (Germany)
 E-mail: klaus.jurkschat@tu-dortmund.de

[d] Prof. Dr. B. Rodríguez-Molina
 Instituto de Química
 Universidad Nacional Autónoma de México
 Ciudad de México 04510 (México)

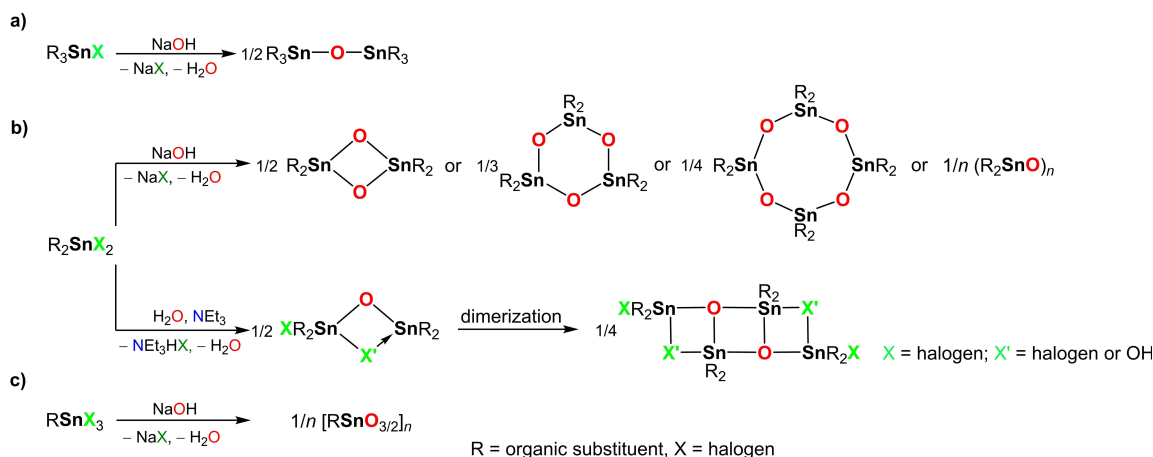
[e] Dr. I. F. Hernández-Ahuactzi
 Centro Universitario de Tonalá, Universidad de Guadalajara
 Av. Nuevo Periférico 555
 Ejido San José Tatepozco, Tonalá, Jalisco 45425 (México)

[f] Prof. Dr. H. Beltrán
 Departamento de Ciencias Básicas, DCBI
 Universidad Autónoma Metropolitana Azcapotzalco
 Ciudad de México 02200 (México)

[*] These authors contributed equally to this work.

Supporting information for this article is available on the WWW under <https://doi.org/10.1002/chem.202101055>

© 2021 The Authors. Chemistry - A European Journal published by Wiley-VCH GmbH. This is an open access article under the terms of the Creative Commons Attribution Non-Commercial NoDerivs License, which permits use and distribution in any medium, provided the original work is properly cited, the use is non-commercial and no modifications or adaptations are made.



Scheme 1. Common base-assisted hydrolysis of tri-, di-, and mono-organotin halides giving a) hexaorganodistannoxanes, b) diorganotin oxides and tetraorganodistannoxanes, and c) mono-organotin sesquioxides. Notes: The organic substituents R (alkyl, alkenyl, alkynyl, aryl) may carry functional groups or not. In the case of the four-, six- and eight-membered rings, the R substituents are bulky, for instance HC(SiMe₃)₂ and tBu.

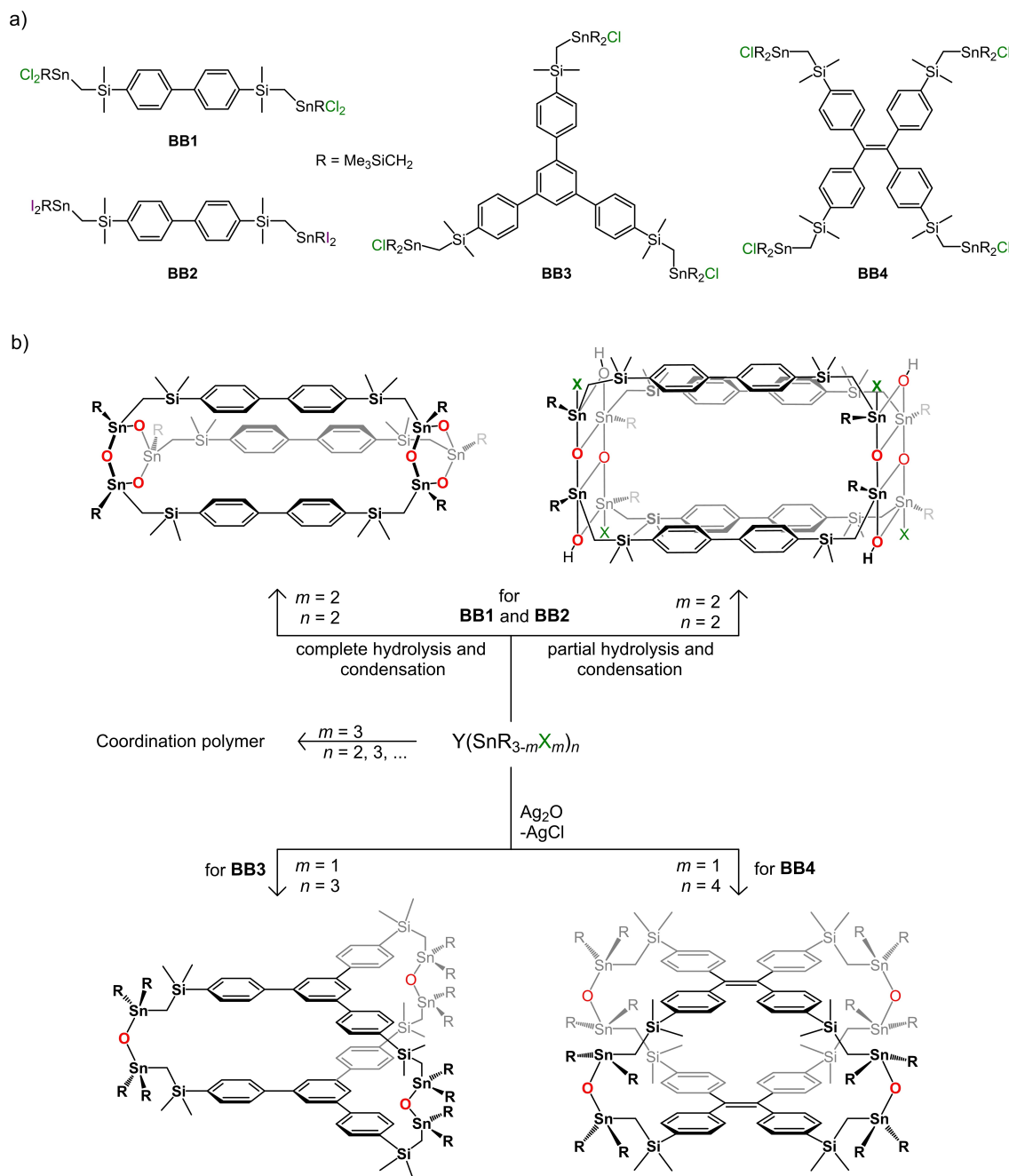
corresponding organotin oxides is a convenient route for the generation of cage compounds.

The tin atoms in triorganotin precursors are susceptible to the formation of single Sn–O–Sn (μ -oxo) bridges (Scheme 1a);^[34–35] therefore, with di- and oligo-nuclear specimens macrocyclic or cage-type structures could be expected, that is, $[Y(R_2Sn-O-SnR_2)_nY]$ where Y = organic spacer and $n = 2, 3, 4$, etc. In analogy, mononuclear diorganotin fragments are interconnected by the simultaneous formation of two μ -oxo bridges, which leads to the generation of species with four-membered Sn₂O₂,^[36–37] six-membered Sn₃O₃,³⁸ and eight-membered Sn₄O₄ rings or coordination polymers (first row in Scheme 1b).^[39] Starting from di-, tri- and tetranuclear diorganotin tectons and working under conditions of complete hydrolysis of the Sn-halogen bonds, cage compounds or infinite coordination polymers of the general composition $[Y\{Sn(R)(\mu-O)\}_n]_x$ (where Y = organic spacer; $n = 2, 3$, and 4 ; $x = 2, 3, 4, \infty$) would be obtained. Incomplete hydrolysis reactions of diorganotin dihalides give tetraorganodistannoxanes that are usually dimeric, $[R_2XSnOSnX'R_2]_2$ (X = halogen; X' = halogen or OH), in solution and in the solid state showing a ladder-type structure (Scheme 1b).^[30–32] The Sn₄O₂X'₂ core of these ladders consists of three condensed four-membered Sn₂OX'/Sn₂O₂/Sn₂OX' rings. In the presence of dinuclear tin building blocks instead of mononuclear diorganotin reagents, cage-type structures arise (vide infra).^[30–32] Finally, complete hydrolysis and condensation of mono-organotin halides generates organotin oxides of composition $[RnSnO_{3/2}]_{\infty}$, which are usually amorphous coordination polymers (Scheme 1c).^[34–35] From starting materials of higher tin nuclearity, products of composition $[Y(SnO_{3/2})_n]_{\infty}$ (where Y = organic spacer, $n = 2, 3$ and 4) could be formulated, in which each tin atom is bound to three bridging oxygen atoms. In this case 2D or 3D coordination polymers are expected as the resulting products.

The purpose of the present contribution is to illustrate the potential of the building blocks outlined in Scheme 2a (BB1–BB4) for the creation of molecular cages with cavities. Such

cages might be suitable for the inclusion of guest compounds such as aromatics or Lewis bases that can interact with the tin centres. Despite the intense research of organotin compounds,^[40] the strategy of reaction sequences focusing on the interconnection of di- or oligonuclear tin specimens by Sn–O–Sn bond formation is mostly unexplored to date. To the best of our knowledge, so far there is only one report on a molecular cage based on Sn₃O₃ ring formation (such as the cage shown in Scheme 2b, top left), which was isolated upon hydrolysis of 1,4-C₆H₄-[Si(Me)₂CH₂SnRCl₂]₂ with R = –CH–(SiMe₃)₂.^[41] By means of partial hydrolysis of the Sn–X bonds in X₂RSn–Y–SnRX₂ (R = CH₂CMe₃, CH₂CHMe₂, CH₂SiMe₃, Ph; X = Cl, I, OTf; Y = organic spacer group) followed by condensation, a series of cage compounds related to the structure given in Scheme 2b (top right) were obtained, containing two tetranuclear bis(tetraorganodistannoxane) ladders based on the above-described Sn₄O₂X'₂ core. In these cages, pairs of tin oxide clusters are linked between each other by the organic spacer groups attached via Sn–C bonds to the tin atoms (Scheme 2b).^[30–33] The fourfold linkage between the inorganic ladders provides robust inorganic-organic hybrid cages of variable size.^[42–43] In addition, there are reports on a double cage based on the trinuclear fragment $[\{Cl_2RSn(CH_2)_3\}_2SnCl_2]$ (R = CH₂SiMe₃),^[44] on two large macrocyclic assemblies containing belt-type ladders derived from MeSi(CH₂SnRl)₃ (where R = Ph or CH₂SiMe₃),^[45a] on a core-shell type Sn₁₄-oxo cluster,^[45b] on Sn₁₈-oxo wheel nanoclusters,^[45c] high-nuclearity Sn₂₆ and Sn₃₄-oxo clusters,^[45d] and a 24-membered ring containing six triorganotin moieties.^[45e] Finally, there is a limited number of publications on polymeric 2D and 3D organotin oxides based on dinuclear building blocks.^[46–48]

Herein, we report on some preliminary results concerning the above-described strategy towards the achievement of functional organotin cage compounds of variable sizes and shapes based on di-, tri- and tetranuclear organotin halide tectons of composition $[Y(SiMe_2CH_2SnR_{3-m}X_m)_n]$, where Y = 4,4'-biphenylene, 1,3,5-tris(*p*-phenylene)benzene, and 1,1,2,2-tetra-



Scheme 2. a) Building blocks for cage formation through halide-oxide exchange reactions examined herein (**BB1**–**BB4**). b) General outline showing potential cage compounds or 2D/3D coordination polymers based on Sn–O–Sn bridging starting from these di-, tri- or tetranuclear organotin precursors having the general composition $[Y(SnR_{3-m}X_m)]_n$, where Y is an organic linker, and X is a halogen. Note: **BB1**, **BB2** and **BB3** were prepared experimentally in the context of this contribution with R = CH₂SiMe₃. However, R may also be another alkyl or aryl substituent.

kis(*p*-phenylene)ethene; X = Cl or I; $m = 1, 2$; $n = 2, 3, 4$). The tectons **BB1**–**BB3** (R = CH₂SiMe₃) were prepared and used as precursors for the synthesis of the hexa- and octa-nuclear cage compounds 1–3. In addition, for further perspective, the analogous cage resulting from **BB4** (R = Me) was structurally analysed by DFT calculations (Scheme 2).

Results and Discussion

Dinuclear tin tectons and large octanuclear molecular metal cages

The tetrahalogenated dinuclear organotin building blocks **BB1** and **BB2** where R = CH₂SiMe₃ (Scheme 2a) were obtained by four-step synthetic protocols established previously (see Experimental Section in the Supporting Information).^[33] The reaction

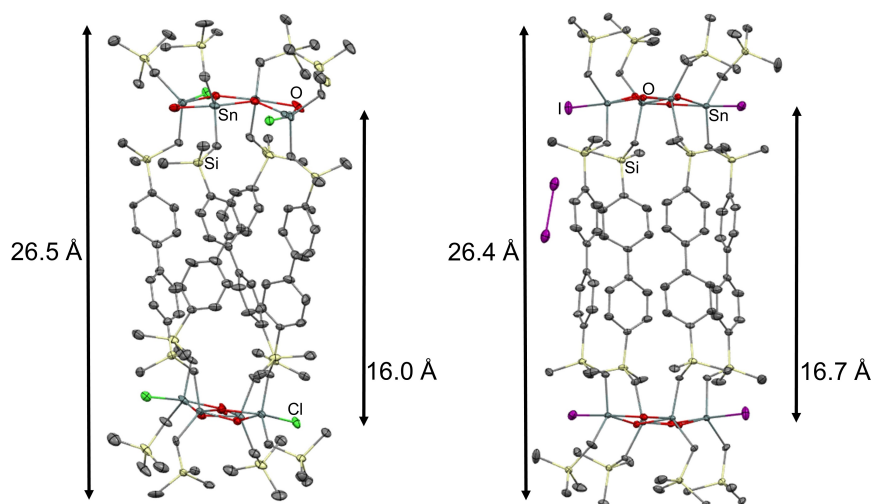


Figure 1. Molecular structures determined by scXRD analysis of compounds **1** (left) and **2·0.48 I₂** (right). Thermal ellipsoids are drawn at the 50% probability level. Hydrogen atoms are omitted for clarity. Colour code: grey (tin), magenta (iodine), green (chlorine), yellow (silicon), red (oxygen) and dark grey (carbon).

of the spacer-bridged bis(diorganotin dichloride) **BB1** with potassium hydroxide, KOH, gave a rather poorly soluble solid material for which the identity could not be established unambiguously. However, extraction of this material with hot THF followed by cooling of the filtrated solution provided single crystals of the cage compound $[(\text{Me}_3\text{SiCH}_2(\text{Cl})\text{SnCH}_2\text{YCH}_2\text{Sn}(\text{OH})\text{CH}_2\text{SiMe}_3)_2(\mu\text{-O})_2]_2$ [**1**, $\text{Y} = p\text{-(Me)}_2\text{SiC}_6\text{H}_4\text{-C}_6\text{H}_4\text{Si}(\text{Me})_2$]. Apparently, the reaction crude contained a mixture of different species, including compound **1** as result of incomplete salt metathesis. In a similar manner, the reaction of the spacer-bridged bis(diorganotin diiodide) **BB2** with KOH gave a solid material almost insoluble in common organic solvents. This material is likely a polymeric organotin oxide precluding NMR spectroscopic studies in solution. Nevertheless, from a dichloromethane solution containing **BB2** and some droplets of distilled water a few single crystals of the co-crystallate $[(\text{Me}_3\text{SiCH}_2(\text{I})\text{SnCH}_2\text{YCH}_2\text{Sn}(\text{OH})\text{CH}_2\text{SiMe}_3)_2(\mu\text{-O})_2]_2 \cdot 0.48 \text{I}_2$ [**2·0.48 I₂**, $\text{Y} = p\text{-(Me)}_2\text{SiC}_6\text{H}_4\text{-C}_6\text{H}_4\text{Si}(\text{Me})_2$] were isolated, after this mixture had been stored for three months. The source of the elemental iodine is unclear. One possibility is that a residual amount of elemental iodine from the synthetic procedure accompanied **BB2**. The diorganotin diiodide derivative **BB2** is an oil, which could not be purified by distillation or chromatography. It was used as obtained from the reaction of $[(\text{Me}_3\text{SiCH}_2(\text{Ph})_2\text{SnCH}_2\text{Si}(\text{Me})_2\text{-}p\text{-C}_6\text{H}_4)_2]$ with elemental iodine, I_2 (see synthetic procedure, Supporting Information).

Compounds **1** and **2·0.48 I₂** were both characterized by single-crystal X-ray diffraction (scXRD) analysis. Figure 1 shows their molecular structures. Table S5 in the Supporting Information) contains crystal and refinement data.

Compound **1** crystallized in the monoclinic space group $P2_1/c$ with two molecules in the unit cell; meanwhile, co-crystal **2·0.48 I₂** crystallized in the triclinic space group $P\bar{1}$ with one molecule in the unit cell.

The structures feature two $[\text{R}(\text{X})\text{Sn}(\mu\text{-O})(\mu\text{-OH})\text{-SnR}]_2$ ladders having a central four-membered Sn_2O_2 ring, a motif that is

included in Scheme 1a. Interestingly, the connectivity among the ladders by means of the organic spacers and the resulting molecular conformations of the cages are quite different, which is also reflected in the difference of the crystallographic symmetry. Cage **1** has twofold rotational symmetry (ca. perpendicular to the long molecule axis) and cage **2** inversion symmetry. In cage **1**, the $p\text{-(Me)}_2\text{SiC}_6\text{H}_4\text{-C}_6\text{H}_4\text{Si}(\text{Me})_2$ connectors crosslink each an *exo*- and an *endo*-tin atom, thus twisting the cage. In contrast, in cage **2**, the organic spacers connect chemically equivalent tin atoms in opposite ladders (Sn_{exo} with Sn_{exo} and Sn_{endo} with Sn_{endo}). This is illustrated in Figure 2, showing that the $[\text{Sn}_4\text{O}_2(\text{OH})_2\text{X}_2]$ ladders are twisted in **1** whilst almost parallel in **2·0.48 I₂**.

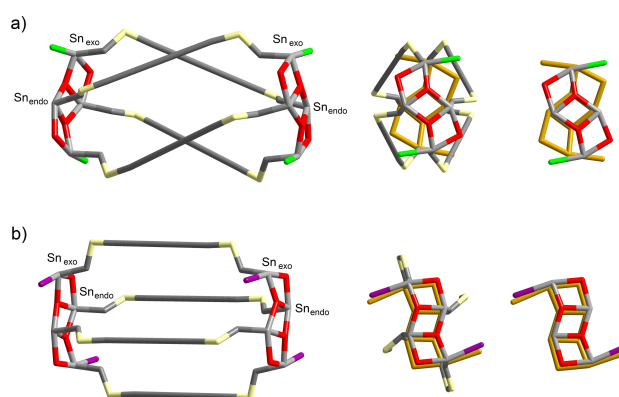


Figure 2. Simplified images of the molecular cages in a) **1** and b) **2·0.48 I₂**, highlighting the differences in the connectivity of the organic spacers between the tin atoms (left) and the mutual orientation of the $[\text{Sn}_4\text{O}_2(\text{OH})_2\text{X}_2]$ fragments within the bis(distannoxane) ladders (middle and right). Colour code: grey (tin), magenta (iodine), green (chlorine), yellow (silicon), red (oxygen) and dark grey (carbon). Notes: Methyl and CH_2SiMe_3 groups as well as hydrogen atoms are omitted for clarity. Biphenylene linkers are represented by single bars. The images on the right show only the $[\text{Sn}_4\text{O}_2(\text{OH})_2\text{X}_2]$ moieties, of which the segment in the background is gold-coloured. The disorder in cage **1** is not shown.

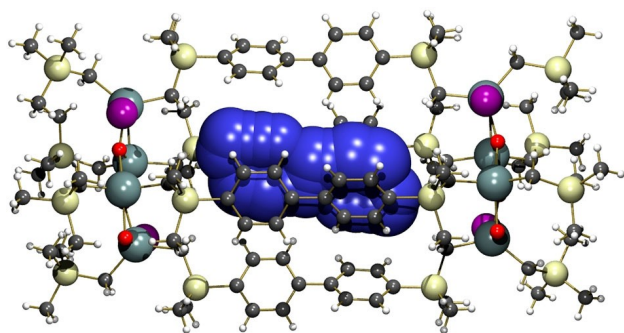


Figure 3. Fragment of the crystal structure of compound $2 \cdot 0.48I_2$, showing the cavity within the molecular cage. Colour code: grey (tin), magenta (iodine), yellow (silicon), red (oxygen), black (carbon) and white (hydrogen).

Concerning the metal coordination environments in **1** and $2 \cdot 0.48I_2$, the endocyclic tin atoms are embedded in C_2O_3 donor sets and exhibit distorted trigonal-bipyramidal geometries, in which the organic substituents and one of the μ -oxo oxygen atoms occupy the equatorial and the remaining oxygen atoms occupy the axial positions. The *exo*-cyclic tin atoms adopt the same coordination geometry, but now one of the axial positions contains a halogen substituent (Cl for **1** and I for $2 \cdot 0.48I_2$). Although the coordination polyhedra at the *endo*- and *exo*-cyclic tin atoms within the bis(distannoxane) ladders have different orientations regarding the distribution of the equatorial and axial sites, the methylene groups of the organic connectors at all four tin atoms are approximately perpendicular to the ladder planes and the $-SiMe_2-$ groups are oriented outwards the cavity. The four connecting organic spacers adopt approximate *gauche*-conformation in **1**, but *syn*-conformation in $2 \cdot 0.48I_2$, as seen from the $-CH_2-Si \cdots Si-CH_2-$ torsion angles (-62.63 and -62.94° for **1**; 2.17 and 2.64° for $2 \cdot 0.48I_2$). In **1**, part of the phenylene rings of the biphenylene connectors are disordered over two positions, indicating mobility even in the solid-state phase. In $2 \cdot 0.48I_2$, this disorder is not observed, but the ellipsoids are significantly enlarged in perpendicular direction with respect to the aromatic ring planes. The centroid \cdots centroid distances between adjacent C_6H_4 -rings are in the range of 4.87 – 5.64 Å in **1** and 5.24 – 6.84 Å in $2 \cdot 0.48I_2$, respectively, indicating the presence of a cavity in the latter case. Difference Fourier maps showed no significant residual electron density in the centre of the molecular cage and the void analysis provided by Platon^[49] revealed an accessible cavity with dimensions of 138 Å³ for $2 \cdot 0.48I_2$ (Figure 3); meanwhile, there was no such void for **1**. The differences among cages **1** and $2 \cdot 0.48I_2$ are eventually a consequence of the incorporation of I_2 molecules in the crystal lattice of $2 \cdot 0.48I_2$. The iodine atoms in the I_2 molecules interact with the tin-bound iodine atoms from two adjacent cage molecules (Figure 4), as established by the $I(1) \cdots I(31)$ distance of $4.028(1)$ Å, which is intermediate between the $I_2 \cdots I_2$ distances observed in solid iodine (3.50 and 4.27 Å).^[50]

In addition, there are two C–H \cdots I contacts with distances of $3.081(1)$ and $3.163(1)$ Å, respectively, being at the border of the

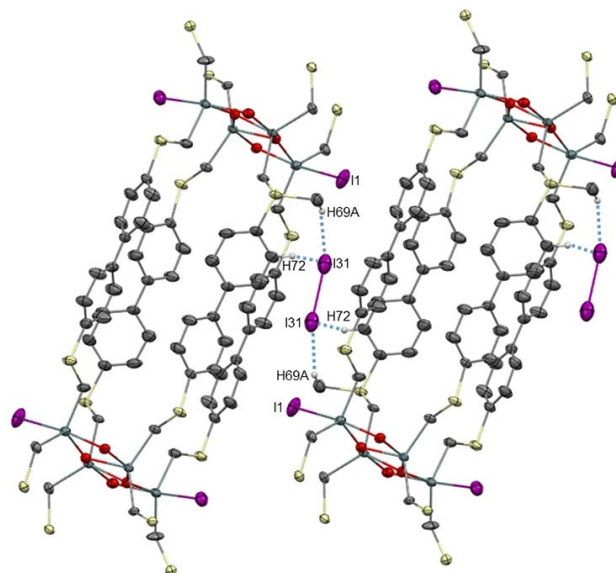


Figure 4. Cut-out of the crystal structure of $2 \cdot 0.48I_2$, showing the I_2 molecules bridging two cages through C–H \cdots I bonding. Note: Thermal ellipsoids are drawn at the 50% probability level. All methyl substituents and hydrogen atoms not involved in hydrogen bonding are omitted for clarity. Colour code: grey (tin), magenta (iodine), yellow (silicon), red (oxygen).

sum of the van der Waals radii^[51–53] (3.08 Å) of the atoms involved.

Previous contributions on double-ladder arrangements based on dinuclear organotin tectons have shown that the choice of the organic connector allows for modifications of geometric features important for potential applications, such as the cavity size and functionality.^[30–32,41–44] As illustrated in Figure 1, opposite tin atoms in compounds **1** and **2** are separated by approximately 16.0 and 16.7 Å, respectively. The latter is the biggest distance so far observed for such double-ladder type compounds, thus representing one of the largest molecular boxes for this class of compounds known to date.^[43] The smallest Sn \cdots Sn distance in such cases (3.6 Å) was observed for the methylene-bridged double ladder $\{[Ph(HO)SnCH_2Sn(I)Ph]O\}_4 \cdot 3CH_2Cl_2$.^[54] The head-to-toe distances of 26.5 (**1**) and 26.4 Å (**2**) are almost equal. In addition, most of the previously reported bis(tetraorganodistannoxane) cages are based on oligomethylene spacers, which are not stable in solution as they are involved in equilibria with single-ladder species.^[43] So far, there are only two reports on analogues with *p*-phenylene-based spacers among the tin atoms, that is, $-CH_2Si(Me)_2-C_6H_4-SiMe_2CH_2-$ ^[38] and $-CH_2CH_2-C_6H_4-CH_2CH_2-$.^[55]

Trinuclear tin tecton and hexanuclear molecular metal cage

The trinuclear building block **BB3** ($R=CH_2SiMe_3$, Scheme 2a) was reported previously^[33] and prepared in analogy to the procedure for the synthesis of **BB1**, using only one molar equivalent of HCl in dichloromethane per tin atom. The reaction in dichloromethane of **BB3** and silver(I) oxide in 2:3 stoichio-

metric ratio yielded the cage compound 1,3,6- $C_6H_3(p-C_6H_4Si(Me)_2CH_2SnR_2OSnR_2CH_2Si(Me)_2C_6H_4-p)_3C_6H_3-1,3,6$ (**3**) as a colourless powder in 90% yield (Scheme S3), as established by elemental analysis, spectroscopic methods (IR and 1D/2D NMR) and mass spectrometry (Figures S22–S33). The 1H , ^{13}C , ^{29}Si and ^{119}Sn NMR spectra in $CDCl_3$ revealed the formation of a highly symmetric and conformationally flexible compound, since only a single set of signals was observed for the reactants involved in its synthesis (Figure 5a–c). The ^{119}Sn NMR chemical shift ($\delta = 133$ ppm) is typical for the expected tetrahedral coordination geometry of the metal atoms. A DOSY NMR experiment for cage **3** in C_6D_6 (Figure 5d) gave a diffusion constant that agrees reasonably well with the expected hydrodynamic molecular volume and molecular weight ($D = 3.48 \times 10^{-10} m^2 s^{-1}$; $r_H = 10.4$ Å; $V_H = 4712$ Å 3 ; $M_W = 3169$ g mol $^{-1}$; $M_{W,calcd} = 2847$ g mol $^{-1}$). In comparison to the starting tecton **BB3** ($D = 4.05 \times 10^{-10} m^2 s^{-1}$; $r_H = 8.9$ Å; $V_H = 2953$ Å 3 ; $MW = 2194$ g mol $^{-1}$; $M_{W,calcd} = 1506$ g mol $^{-1}$), the molecular weight of **3** determined by DOSY is significantly larger, as expected. Moreover, the diffusion coefficient of **3** is comparable to the value reported for a dimeric tetraurea[4]calixarene assembled in C_6D_6 through hydrogen bonding interactions with similar molecular dimensions ($D = 3.2 \times 10^{-10} m^2 s^{-1}$; $M_W = 3152$ g mol $^{-1}$).^[56] The cage assembly could be detected also by two different mass spectrometric measurements, that is, ESI $^+$ and DART (Figures S30–S33). The ESI $^+$ mass spectrum revealed clusters at m/z 2849 and 2866 with characteristic patterns for a hexanuclear tin species. The peak intensity distribution in the experimental mass clusters, according to compositions with the different

isotopes of the elements, are in good agreement with the patterns simulated for $[M+H]^+$ and $[M+NH_4]^+$. In addition, the mass cluster at m/z 1424 contains peaks indicative of the twofold charged molecular ion (Figure S31).

Single crystals suitable for scXRD analysis could not be obtained; therefore, the molecular structure of a slightly modified version of cage **3** (i.e., **3'** with $SnMe_2$ groups instead of $Sn(CH_2SiMe_3)_2$ moieties) was geometry-optimized by DFT calculations using the B3LYP functional and the def2-SVP basis set following approaches for previously reported organotin macrocycles and cages.^[33,57] As seen from Figure 6a, the cage adopts the shape of a triangular prism. The molecular dimensions of this cage are illustrated by the Sn...Sn distances forming the edges of the polyhedron, viz., 17.99–18.13 Å for the triangular and 3.75–3.76 Å for the Sn–O–Sn fragments. There is a cavity in the centre of the cage suitable for the inclusion of aromatic guest compounds, as illustrated by the centroid...centroid distance of 7.87 Å between the central C_6H_3 rings. Considering that the Sn–O–Sn fragments might be replaced by Sn–X–Sn units, where X is a larger atom or bidentate bridging function (e.g., S^{2-} , Se^{2-} , HPO_4^{2-} , CO_3^{2-} , etc.), an interesting series of cage compounds with variable cavity size would become available.

Tetranuclear tin tecton and octanuclear molecular metal cage

As a perspective for future work, a simplified version of the tetranuclear molecular cage that is expected from the hydrolysis and condensation reaction of **BB4** (Scheme 2a) was

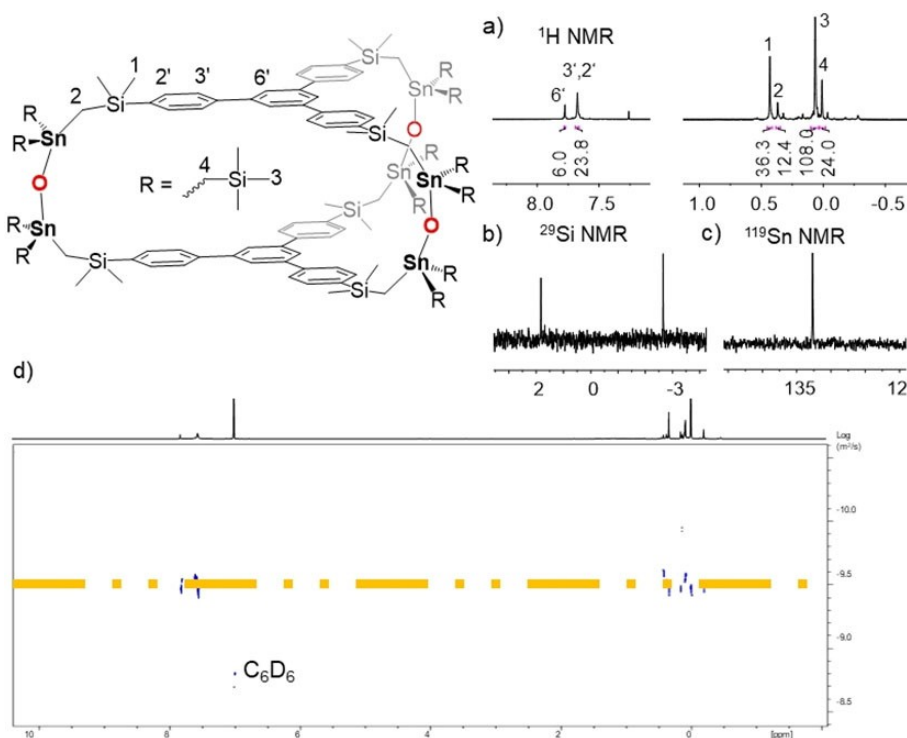


Figure 5. NMR experiments of a solution of cage **3** in $CDCl_3$: a) Integrated 1H NMR, b) $^{29}Si\{^1H\}$ NMR, c) $^{119}Sn\{^1H\}$ NMR and d) diffusion-ordered 1H NMR (DOSY, in C_6D_6).

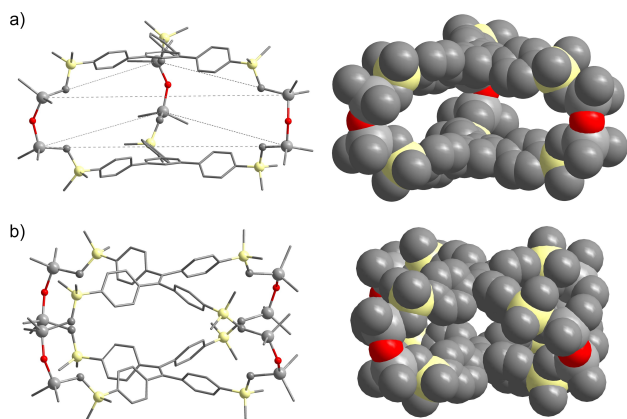


Figure 6. Geometry-optimized (B3LYP/def2-SVP) molecular structures in the gas phase for cage compounds a) 3' and b) 4'. Colour code: grey (tin), yellow (silicon), red (oxygen), grey (carbon) and white (hydrogen). Note: The dotted lines in the molecular structure of 3' indicate the trigonal prism formed by the tin atoms.

modelled by DFT methods in analogy to compound 3'. The calculated molecular structure of 4' is given in Figure 6b, showing the expected cuboid-type molecular structure. The Sn...Sn distances resulted 10.41–10.55, 15.77–15.83 and 3.74 Å, with the first two sets of values corresponding to the metal-metal separations generated by the organic connector. The Sn...Sn distance for the Sn–O–Sn entities is similar to the value observed in cage 3', thus resulting in a similar cavity height (centroid...centroid distance between opposite ethylene units = 7.04 Å). Nevertheless, due to the torsion of the C₆H₄ rings, the accessible cavity size is significantly reduced.

Conclusions

The combined experimental/theoretical approach outlined in this contribution shows that di-, tri- and tetranuclear organotin mono- and dihalides are building blocks suitable for the generation of large oligonuclear cage compounds via simple reactions with water and/or potassium hydroxide or silver oxide. The circumstance that the examples described herein use organometallic tectons which are then linked by an *inorganic* ligand constitutes in a certain way an alternative or, better said, inverted strategy to the generally employed method of forming metal-containing supramolecular assemblies, viz., the combination of single-metal nodes or secondary building units with di- or oligofunctional *organic* ligands.

Nevertheless, the results presented herein show that diorganotin dihalide tectons are susceptible to the formation of the intermediate distannoxane ladders instead of the complete hydrolysis product, which is a handicap for applications as molecular containers due to their limited solubility. However, for the triorganotin monohalide tectons explored herein, the halide/oxide exchange proceeded as expected, thus indicating that this route might be more efficient for the directed formation of cage compounds.

The organic substituents attached to the tin atoms provide the cage molecules with the feature that subsequent or preliminary structural modifications can be carried out; this is relevant for the variation of physical/chemical properties and the generation of functional molecular containers. Currently, more sophisticated oligonuclear organotin building blocks are being designed in our laboratories together with the development of other efficient strategies for the generation of cages based on connections through metal-ligand-metal bonds.

Experimental Section

For the synthesis and complete characterization of the organotin building blocks and the assemblies achieved by hydrolysis, see the Supporting Information.

Deposition numbers 2071224 and 2071225 contain the supplementary crystallographic data for this paper. These data are provided free of charge by the joint Cambridge Crystallographic Data Centre and Fachinformationszentrum Karlsruhe Access Structures service www.ccdc.cam.ac.uk/structures.

Acknowledgements

Financial support from Consejo Nacional de Ciencia y Tecnología (CONACyT) through project no. 158098 and 229929 is gratefully acknowledged. The authors thank Ing. Victoria Labastida-Galván (LANEM, UAEM), Dra. Rosa Santillan, and Dr. Robert B. Cody (Jeol USA, Inc.) for acquisition and assistance in the interpretation of the mass spectra. Open access funding enabled and organized by Projekt DEAL.

Conflict of Interest

The authors declare no conflict of interest.

Keywords: DFT calculations · DOSY NMR spectroscopy · metallacycles · tetraorganodistannoxane · X-ray diffraction

- [1] J. M. Lehn, *Chem. Soc. Rev.* **2007**, *36*, 151–160.
- [2] E. G. Percástegui, J. Mosquera, J. R. Nitschke, *Angew. Chem. Int. Ed.* **2017**, *56*, 9136–9140; *Angew. Chem.* **2017**, *129*, 9264–9268.
- [3] A. D. Chavez, A. M. Evans, N. C. Flanders, R. P. Bisbey, E. Vitaku, L. X. Chen, W. R. Dichtel, *Chem. Eur. J.* **2018**, *24*, 3989–3993.
- [4] K. Severin, R. Scopelliti, M. Pappmeyer, C. Schouwey, *Dalton Trans.* **2015**, *44*, 2252–2258.
- [5] R. Custelcean, *Chem. Soc. Rev.* **2014**, *43*, 1813–1824.
- [6] M. Mastalerz, *Angew. Chem. Int. Ed.* **2010**, *49*, 5042–5053; *Angew. Chem.* **2010**, *122*, 5164–5175.
- [7] H. Jędrzejewska, M. Wierzbicki, P. Cmoch, K. Rissanen, A. Szumna, *Angew. Chem. Int. Ed.* **2014**, *53*, 13760–13764; *Angew. Chem.* **2014**, *126*, 13980–13984.
- [8] A. R. Stefankiewicz, E. Tamanini, G. D. Pantoş, J. K. M. Sanders, *Angew. Chem. Int. Ed.* **2011**, *50*, 5725–5728; *Angew. Chem.* **2011**, *123*, 5843–5846.
- [9] M. Zhang, M. L. Saha, M. Wang, Z. Zhou, B. Song, C. Lu, X. Yan, X. Li, F. Huang, S. Yin, P. J. Stang, *J. Am. Chem. Soc.* **2017**, *139*, 5067–5074.
- [10] B. M. Schmidt, T. Osuga, T. Sawada, M. Hoshino, M. Fujita, *Angew. Chem. Int. Ed.* **2016**, *55*, 1561–1564; *Angew. Chem.* **2016**, *128*, 1587–1590.

- [11] C. J. Brown, F. D. Toste, R. G. Bergman, K. N. Raymond, *Chem. Rev.* **2015**, *115*, 3012–3035.
- [12] K. M. Choi, D. Kim, B. Rungtaweivoranit, C. A. Trickett, J. T. D. Barmanbek, A. S. Alshammari, P. Yang, O. M. Yaghi, *J. Am. Chem. Soc.* **2017**, *139*, 356–362.
- [13] P. Brunet, M. Simard, J. D. Wuest, *J. Am. Chem. Soc.* **1997**, *119*, 2737–2738.
- [14] M. W. Hosseini, *Acc. Chem. Res.* **2005**, *38*, 313–323.
- [15] P. J. Stang, *Chem. Eur. J.* **1998**, *4*, 19–27.
- [16] D. Fujita, Y. Ueda, S. Sato, N. Mizuno, T. Kumasaka, M. Fujita, *Nature* **2016**, *540*, 563–566.
- [17] M. Eddaoudi, D. B. Moler, H. Li, B. Chen, T. M. Reineke, M. O’Keeffe, O. M. Yaghi, *Acc. Chem. Res.* **2001**, *34*, 319–330.
- [18] X. Sun, D. W. Johnson, D. L. Caulder, R. E. Powers, K. N. Raymond, E. H. Wong, *Angew. Chem. Int. Ed.* **1999**, *38*, 1303–1307; *Angew. Chem.* **1999**, *111*, 1386–1390.
- [19] X. Sun, D. W. Johnson, D. L. Caulder, K. N. Raymond, E. H. Wong, *J. Am. Chem. Soc.* **2001**, *123*, 2752–2763.
- [20] K. C. Kumara Swamy, C. G. Schmid, R. O. Day, R. R. Holmes, *J. Am. Chem. Soc.* **1990**, *112*, 223–228.
- [21] V. Chandrasekhar, P. Thilagar, J. F. Bickley, A. Steiner, *J. Am. Chem. Soc.* **2005**, *127*, 11556–11557.
- [22] R. Reyes-Martinez, P. García y García, M. Lopez-Cardoso, H. Höpfl, H. Tlahuext, *Dalton Trans.* **2008**, 6624–6627.
- [23] E. Dornsiepen, F. Dobener, S. Chatterjee, S. Dehnen, *Angew. Chem. Int. Ed.* **2019**, *58*, 17041–17046; *Angew. Chem.* **2019**, *131*, 17197–17202.
- [24] E. Dornsiepen, F. Weigend, S. Dehnen, *Chem. Eur. J.* **2019**, *25*, 2486–2490.
- [25] E. Geringer, M. Gerhard, M. Koch, C. K. Krug, J. M. Gottfried, S. Dehnen, *Chemistry* **2021**, *27*, 2734–2741.
- [26] Z. Hassanzadeh Fard, M. R. Halvagar, S. Dehnen, *J. Am. Chem. Soc.* **2010**, *132*, 2848–2849.
- [27] M. R. Halvagar, Z. Hassanzadeh Fard, S. Dehnen, *Chem. Eur. J.* **2011**, *17*, 4371–4374.
- [28] Z. You, K. Harms, S. Dehnen, *Eur. J. Inorg. Chem.* **2015**, 5322–5328.
- [29] K. Hanau, N. Rinn, M. Argentari, S. Dehnen, *Chem. Eur. J.* **2018**, *24*, 11711–11716.
- [30] D. Dakternieks, K. Jurkschat, D. Schollmeyer, H. Wu, *Organometallics* **1994**, *13*, 4121–4123.
- [31] M. Mehring, M. Schürmann, I. Paulus, D. Horn, K. Jurkschat, A. Orita, J. Otera, D. Dakternieks, A. Duthie, *J. Organomet. Chem.* **1999**, *574*, 176–192.
- [32] M. Mehring, I. Paulus, B. Zobel, M. Schürmann, K. Jurkschat, A. Duthie, D. Dakternieks, *Eur. J. Inorg. Chem.* **2001**, 153–160.
- [33] I. Rojas-León, H. Alnasr, K. Jurkschat, M. G. Vasquez-Ríos, I. F. Hernández-Ahuactzi, H. Höpfl, *Chem. Eur. J.* **2018**, *24*, 4547–4551.
- [34] R. K. Ingham, S. D. Rosenberg, H. Gilman, *Chem. Rev.* **1960**, *60*, 459–539.
- [35] V. Chandrasekhar, S. Nagendran, V. Baskar, *Coord. Chem. Rev.* **2002**, *235*, 1–52.
- [36] V. K. Belsky, N. N. Zemlyansky, I. V. Borisova, N. D. Kolosova, I. P. Beletskaya, *J. Organomet. Chem.* **1983**, *254*, 189–192.
- [37] M. A. Edelman, P. B. Hitchcock, M. F. Lappert, *J. Chem. Soc. Chem. Commun.* **1990**, 1116–1118.
- [38] H. Puff, W. Schuh, R. Sievers, W. Wald, R. Zimmer, *J. Organomet. Chem.* **1984**, *260*, 271–280.
- [39] B. Zobel, M. Schürmann, K. Jurkschat, D. Dakternieks, A. Duthie, *Organometallics* **1998**, *17*, 4096–4104.
- [40] A. G. Davies, M. Gielen, K. H. Pannell, E. R. T. Tiekink, *Tin Chemistry: Fundamentals, Frontiers and Applications*, Wiley, Chichester, **2008**.
- [41] J. Beckmann, B. Zobel, K. Jurkschat, M. Schürmann, E. R. T. Tiekink, *Organometallics* **2003**, *22*, 1343–1345.
- [42] D. Dakternieks, A. Duthie, B. Zobel, K. Jurkschat, M. Schürmann, E. R. T. Tiekink, *Organometallics* **2002**, *21*, 647–652.
- [43] J. Beckmann, D. Dakternieks, A. Duthie, F. S. Kuan, K. Jurkschat, M. Schürmann, E. R. T. Tiekink, *New J. Chem.* **2004**, *28*, 1268–1276.
- [44] M. Mehring, M. Schürmann, H. Reuter, D. Dakternieks, K. Jurkschat, *Angew. Chem. Int. Ed. Engl.* **1997**, *36*, 1112–1114; *Angew. Chem.* **1997**, *109*, 1150–1152.
- [45] a) J. Ayari, C. R. Göb, I. M. Oppel, M. Lutter, W. Hiller, K. Jurkschat, *Angew. Chem. Int. Ed.* **2020**, *59*, 23892–23898; *Angew. Chem.* **2020**, *132*, 24102–24109; b) Y. Zhu, J. Zhang, L. Zhang, *Chem. Commun.* **2020**, *56*, 1433–1435; c) Y. Zhu, Q. Li, D. Li, J. Zhang, L. Zhang, *Chem. Commun.* **2021**, *57*, 5159–5162; d) Y. Zhu, L. Zhang, J. Zhang, *Chem. Sci.* **2019**, *10*, 9125–2129; e) Yuan-Yuan Zhang, R.-F. Zhang, S.-L. Zhang, S. Cheng, Q.-L. Lia, C.-L. Ma, *Dalton Trans.* **2016**, *45*, 8412–8421.
- [46] H. Elhamzaoui, B. Jousseau, H. Riague, T. Toupance, P. Dieudonné, C. Zakri, M. Maugey, H. Allouchi, *J. Am. Chem. Soc.* **2004**, *126*, 8130–8131.
- [47] H. Elhamzaoui, B. Jousseau, T. Toupance, C. Zakri, M. Biesemans, R. Willem, H. Allouchi, *Chem. Commun.* **2006**, 1304–1306.
- [48] T. Toupance, H. El Hamzaoui, B. Jousseau, H. Riague, I. Saadeddin, G. Campet, J. Brötz, *Chem. Mater.* **2006**, *18*, 6364–6372.
- [49] P. van der Sluis, A. L. Spek, *Acta Crystallogr. Sect. A* **1990**, *64*, 194–201.
- [50] A. F. Holleman, E. Wiberg, N. Wiberg, *Lehrbuch der anorganischen Chemie*, 34th ed., Walter de Gruyter, Berlin, **1995**.
- [51] A. Bondi, *J. Phys. Chem.* **1964**, *68*, 441–451.
- [52] R. S. Rowland, R. Taylor, *J. Phys. Chem.* **1996**, *100*, 7384–7391.
- [53] M. Mantina, A. C. Chamberlin, R. Valero, C. J. Cramer, D. G. Truhlar, *J. Phys. Chem. A* **2009**, *113*, 5806–5812.
- [54] M. Mehring, G. Gabriele, S. Hadjikakou, M. Schürmann, D. Dakternieks, K. Jurkschat, *Chem. Commun.* **2002**, 834–835.
- [55] D. Dakternieks, A. Duthie, B. Zobel, K. Jurkschat, M. Schürmann, E. R. T. Tiekink, *Organometallics* **2002**, *21*, 647–652.
- [56] L. Frish, S. E. Matthews, V. Böhmer, Y. Cohen, *J. Chem. Soc. Perkin Trans. 2* **1999**, 669–671.
- [57] A. Torres-Huerta, J. Cruz-Huerta, H. Höpfl, L. Hernández-Vázquez, J. Escalante-García, A. Jiménez-Sánchez, R. Santillan, I. Hernández-Ahuactzi, M. Sánchez, *Inorg. Chem.* **2016**, *55*, 12451–12469.

Manuscript received: March 23, 2021

Accepted manuscript online: June 2, 2021

Version of record online: June 23, 2021